Heat transfer in a liquid fluidized bed
by Sambasiva Rao Uppala

A thesis submitted to the Graduate Faculty in partial fulfillment of the requirements for the degree of
MASTER OF SCIENCE in Chemical Engineering
Montana State University

Abstract:
Local and average heat transfer coefficients for heat transfer from an electrically heated internal tube to a water fluidized bed were investigated. Three types of particles were used in this study. Glass spheres of 0.0185-inch average diameter, coke particles of 0.014-inch average diameter and stainless steel particles of 0.014-inch average diameter were used. A movable thermocouple was fitted inside the heated tube to measure the tube's wall temperature at any vertical height. Bulk fluid temperatures were determined with protected thermocouples placed at five locations in the bed.

Variables studied included particle size, shape, and concentration, and liquid mass velocity. Average heat transfer coefficients over the fluidized bed were correlated with an equation based on a particle mode heat transfer mechanism. Local heat transfer coefficients were estimated at five different locations.

The results of this investigation are as follows: (l) Local heat transfer coefficients show a progressive increase with mass velocity. A decrease is observed in the local heat transfer coefficient with distance from the entrance of the tube. (2) For fluidization, the average Nusselt number is correlated with an equation based on a particle mode heat transfer mechanism.

In presenting this thesis in partial fulfillment of the requirements for an advanced degree at Montana State University, I agree that the Library shall make it freely available for inspection. I further agree that permission for extensive copying of this thesis for scholarly purposes may be granted by my major professor, or, in his absence, by the Director of Libraries. It is understood that any copying or publication of this thesis for financial gain shall not be allowed without my written permission.

Signature [illegible]

Date October 2, 1969

HEAT TRANSFER IN A LIQUID FLUIDIZED BED

by

SAMBASIVA RAO UPPALA

A thesis submitted to the Graduate Faculty in partial fulfillment of the requirements for the degree

of

MASTER OF SCIENCE

in

Chemical Engineering

Approved:

Lloyd Berg
Head, Major Department

William J. Genetti
Chairman, Examining Committee

K. Goering
Graduate Dean

MONTANA STATE UNIVERSITY
Bozeman, Montana

December, 1969

ACKNOWLEDGEMENT

The author wishes to express his gratitude to Dr. William E. Genetti for his assistance and encouragement throughout the duration of the investigation, and to Dr. R. L. Nickelson, Dr. F. P. McCandless and Dr. R. E. Lund for being on his graduate committee. He would like to thank Mr. Cy Huso and Mr. Jim Tillery for their assistance in the construction of the equipment. He would also like to thank the Chemical Engineering Department at Montana State University for its financial support.

TABLE OF CONTENTS

LIST OF TABLES

LIST OF FIGURES

ABSTRACT

Local and average heat transfer coefficients for heat transfer from an electrically heated internal tube to a water fluidized bed were investigated. Three types of particles were used in this study. Glass spheres of 0.0185-inch average diameter, coke particles of 0.014-inch average diameter and stainless steel particles of 0.014-inch average diameter were used. A movable thermocouple was fitted inside the heated tube to measure the tube's wall temperature at any vertical height. Bulk fluid temperatures were determined with protected thermocouples placed at five locations in the bed.

Variables studied included particle size, shape, and concentration, and liquid mass velocity. Average heat transfer coefficients over the fluidized bed were correlated with an equation based on a particle mode heat transfer mechanism. Local heat transfer coefficients were estimated at five different locations.

The results of this investigation are as follows: (1) Local heat transfer coefficients show a progressive increase with mass velocity. A decrease is observed in the local heat transfer coefficient with distance from the entrance of the tube. (2) For fluidization, the average Nusselt number is correlated with an equation based on a particle mode heat transfer mechanism.

$$Nu_p = \frac{2\phi\,(1-\varepsilon)^{-0.85}}{\left[\,1+\frac{102}{Re_p^{0.43}}\left(\frac{K_\ell}{\rho_s C_s g^{0.5} D_p^{1.5}}\right)\left(\frac{\rho_s}{\rho_\ell}\right)^{0.8}\,\right]^2}$$

INTRODUCTION

One of the many devices developed in recent years to handle the industrial process heat transfer efficiently is the fluidized bed. Some of the devices used to decrease the resistance to heat transfer include: rough surfaces, extended surfaces, and baffled tubular heat exchangers. The phenomenon of heat transport in fluidized beds has been the subject of numerous studies in the past two decades because of the many desirable characteristics of fluidized-bed heat transfer and the increased application of fluidized-bed reactors.

Fluidization is the operation by which fine solids are transformed into a fluid-like state through contact with a gas or liquid. When fluid is passed through a bed of fine particles, there is a certain velocity when the particles are suspended in the upward flowing gas or liquid. The bed is then considered to be just fluidized and is referred to as a bed at minimum fluidization. In liquid-solid systems, an increase in flow rate above minimum fluidization usually results in a smooth, progressive expansion of the bed. A bed such as this is called a particulately fluidized bed, a homogeneously fluidized, or simply a liquid fluidized bed.

The presence of solids greatly increases the heat transfer rates from a surface to a liquid fluidized bed. This is attributed to the increased turbulance the fluidized bed offers, as well as the energy transfered by solids in contact with the surface.

This investigation is a study of local and average heat transfer rates from an electrically heated surface to the fluidized bed. Heater surface temperatures were measured by a moving thermocouple probe inside an electrically heated tube. Surface temperatures and bulk temperatures made it possible to calculate local heat transfer coefficients at different places along the tube and for different liquid flow rates and particle concentrations.

LITERATURE SURVEY

Proposed Fluidized Bed Heat Transfer Mechanisms

Several theoretical mechanisms to describe the fluidized bed heat transfer were proposed. Extensive descriptions of these are given by Leva (7), Kunii and Levenspiel (5), Genetti (2) and Zenz and Othmer (11). One of the mechanisms proposed was the particle mode heat transfer mechanism by Zieglar, Koppel and Brazelton (12). A modified particle mode heat transfer mechanism for gas fluidized beds was proposed by Genetti and Knudsen (3). The mechanism that is being applied to liquid fluidized bed heat transfer in the present investigation is similar to that presented by Genetti and Knudsen. The details and modifications of this mechanism are discussed at the end of this section.

Experimental Study of Fluidized Bed Heat Transfer

The experimental study of liquid fluidized bed heat transfer is meager compared to the work done in the case of gas fluidized bed heat transfer. The experimental studies of the latter were summarized by Leva (7), Kunii and Levenspiel (5) and Genetti (2).

The experimental study of fluidized bed heat transfer has been broken down into two categories: Particle-to-Fluid Heat Transfer and Surface-to-Fluidized-Bed Heat Transfer.

Particle-to-Fluid Heat Transfer:

In a fluidized bed the particles serve as energy carriers. The

particles gain energy at the heat transfer surface and release it to the fluid phase. In particle-to-fluid heat transfer, one is interested in the rate of heat transfer from the particle to the fluid. Studies on heat transfer between solid particles and fluidizing medium are necessary mainly to elucidate the mechanism of dissipation of heat of reaction, heat of dilution, etc., in a fluidized bed, and also in fluidized bed reactor design.

Sunkoori and Kaparthi (10) fluidized heated quartz and granite particles of different sizes in a water fluidizing medium. They measured heat transfer coefficients between the particles and the fluidizing medium under unsteady state conditions. Heat transfer coefficients varying from 113 to 620 Btu/hr.ft.^{2}°F were obtained and they noticed an increase in heat transfer rates with particle diameter and mass velocity. They correlated their data with the following equation:

$$\frac{h_p D_p}{K} = 0.00391\left(\frac{D_p G}{\mu}\right)^{2.1} \qquad (1)$$

More recently Holman, Moore and Wang (4) measured particle-to-fluid heat transfer coefficients for stainless steel and lead spheres fluidized in a water medium. The spheres were heated by an induction heating field. These authors correlated the particle Nusselt numbers with the following equation:

$$Nu_p = 1.28 \times 10^{-5} (Re_p F_\varepsilon)^{2.0} Pr^{0.67} \left(\frac{D_t}{D_p}\right)^{0.5} \left(\frac{\rho_f}{\rho_s}\right)^2 \left(\frac{\mu}{\mu_o}\right)^{0.83} \qquad (2)$$

The velocity correction factor, F_ε, was used to account for variation in porosity.

Surface-to-Fluidized-Bed Heat Transfer:

Lemlich and Caldas (6) fluidized glass particles of different sizes in a liquid medium. Heat transfer rates from the external, heated wall were measured. A maximum in heat transfer coefficient was obtained for each particle size. They identified two flow regimes; below the mass velocity, corresponding to the maximum heat transfer coefficient, another above the mass velocity, also corresponding to the maximum heat transfer coefficient. They have proposed correlations for respective regimes.

For low velocity fluidization the correlation is as follows:

$$Nu_p = 0.055\ Re_p \tag{3}$$

For high velocity fluidization the following equation was proposed:

$$j = (St)(Pr)^{2/3} = 1.4\left(\frac{D_t}{D_p}\right)^{0.79}/Re_t\varepsilon \tag{4}$$

Richardson and Mitson (9) measured the coefficients for the transfer of heat to a liquid-solid fluidized system and they found that the presence of solids can increase the coefficients by a factor of up to five. They correlated their data with the following equation:

$$Nu = 55\ Pr^{0.4}\left(\frac{C_s}{C_\ell}\right)^{0.28}\left(\frac{\rho_\ell V_i D_p}{\mu_\ell}\right)^N \tag{5}$$

where:
$$N = 0.020\left(\frac{\rho_s}{\rho_\ell} + 3.45\right) \tag{5a}$$

Presently proposed Heat Transfer Mechanism:

The model that is proposed here is an extension of the model proposed by Genetti and Knudsen (2,3) for gas fluidized bed heat transfer.

This model is formulated under the assumption that particles are spheres of uniform diameter. Furthermore, particles from the bulk of the fluidized bed are assumed to move adjacent to the transfer surface, while close to the surface, the particle receives energy by convection from the fluid around it. After some time the particle leaves the surface and returns to the bulk of the bed. The major portion of heat transfer is assumed to occur by this mechanism, while conductive and radiative heat transfer is negligible. Based on this mechanism, the boundary value problem is solved, and under the assumptions which are still valid for the case of liquids, the time average heat transfer rate is obtained as:

$$q_p = \frac{\pi D_p K_\ell (T_w - T_b)}{(1 + \frac{M\bar{\theta}}{2})^2} \tag{6}$$

where: $$M = \frac{12K_\ell}{\rho_s C_s D_p^2} \quad \text{and} \tag{6a}$$

$\bar{\theta}$ = the average contact time.

In order to obtain an expression for the heat transfer flux based on the wall surface, the number of particles at the surface per unit area will have to be derived. The number of particles per unit area, γ_p, will be related to the particle fraction $(1-\varepsilon)$, and the particle diameter. A relation of the following form has been proposed:

$$\gamma_p = K_1(1-\varepsilon)^{-0.85} f(D_p) \tag{7}$$

It is experimentally observed that the heat transfer coefficient is dependent on particle fraction in the manner assumed in Equation 7.

For a completely covered surface with hexagonal packing, γ_p and $(1-\varepsilon)$ are:

$$\gamma_p = \frac{2/\sqrt{3}}{D_p^2} \tag{8}$$

$$(1-\varepsilon) = 14/27 \tag{9}$$

therefore: $K_1 = 0.637$ and (10)

$$f(D_p) = \frac{1}{D_p^2} \tag{11}$$

By substituting Equations 10 and 11 into Equation 7, we get the following equation for γ_p:

$$\gamma_p = \frac{0.637\ (1-\varepsilon)^{-0.85}}{D_p^2} \tag{12}$$

By multiplying q_p by γ_p, we can write an equation for the heat flux from the wall surface, i.e.,

$$q = \gamma_p q_p = \frac{2.0\ (1-\varepsilon)^{-0.85}\ (T_w - T_b)}{D_p \left(1 + \frac{6K_\ell \bar{\theta}}{\rho_s C_s D_p^2}\right)^2} \tag{13}$$

The particle Nusselt number is:

$$Nu_p = \frac{2.0\ (1-\varepsilon)^{-0.85}}{\left(1 + \frac{6K_\ell \bar{\theta}}{\rho_s D_s D_p^2}\right)^2} \tag{14}$$

The average contact time would be affected by the following variables:

1. particle diameter, D_p
2. particle density, ρ_s
3. liquid density, ρ_ℓ
4. liquid viscosity, μ
5. acceleration due to gravity, g
6. mass velocity, G

With the aid of dimensional analysis the following dimensionless groups can be obtained:

$$\left(\frac{\rho_s}{\rho_\ell}\right), \qquad \left(\frac{\bar{\theta}\, g^{1/2}}{D_p^{1/2}}\right), \qquad \left(\frac{D_p G}{\mu}\right)$$

With these groups an equation of the following form for $\bar{\theta}$ is obtained:[1]

$$\bar{\theta} = C_1 \left(\frac{D_p}{g}\right)^{1/2} Re_p^e \left(\frac{\rho_s}{\rho_\ell}\right)^f \tag{15}$$

The exponents in this equation have to be determined experimentally. Substituting Equation 15 in Equation 14 the following is obtained:

$$Nu_p = \frac{2.0\,(1-\varepsilon)^{-0.85}}{\left[1+\frac{6K_\ell}{\rho_s C_s D_p^2}\, C_1 \left(\frac{D_p}{g}\right)^{1/2} Re_p^e \left(\frac{\rho_s}{\rho_\ell}\right)^f\right]^2} \tag{16}$$

1. It would be expected that the average contact time, $\bar{\theta}$, would also depend on the particle fraction, $(1-\varepsilon)$, however, no such dependence was observed experimentally in the correlation obtained.

EXPERIMENTAL EQUIPMENT

The experimental equipment was designed in order to determine local and average heat transfer coefficients from an internal heat source to a liquid fluidized bed. The components of the equipment included a fluidizing unit, a pump, a power source and the measuring devices. The general set-up of the equipment is shown in Figure 1.

The Fluidizing Unit

The fluidizing unit consisted of a 2 1/2-inch I.D., two feet long, cast acrylic tube. The thickness of the tube wall was 1/8-inch. At the top and bottom it was fitted with flanges of 3/4-inch thickness. Over the top flange was fitted a rubber gasket and a circular plate made of micarta. The top plate and the top flange were tightened with bolts to ensure air-tightness. Four openings of 1/2-inch diameter were made around the tube at 1 1/2-inches from the top of the tube to serve as the outlet for the fluid. The four outlets were connected by the use of T-junctions and a single tube carried the water to the tank.

To the bottom flange affixed to the tube, another flange of the same dimensions was attached by bolts, with a gasket in-between. Between the flanges was placed a perforated circular iron plate, over which a 200 mesh wire screen was affixed. This plate held the particles in the bed. The intake piping was attached to the flange.

A 321 stainless steel tube, 3/4-inch O.D., 0.012-inch thick and 30-inches long, was fitted through the center of the bed. Electrical wire

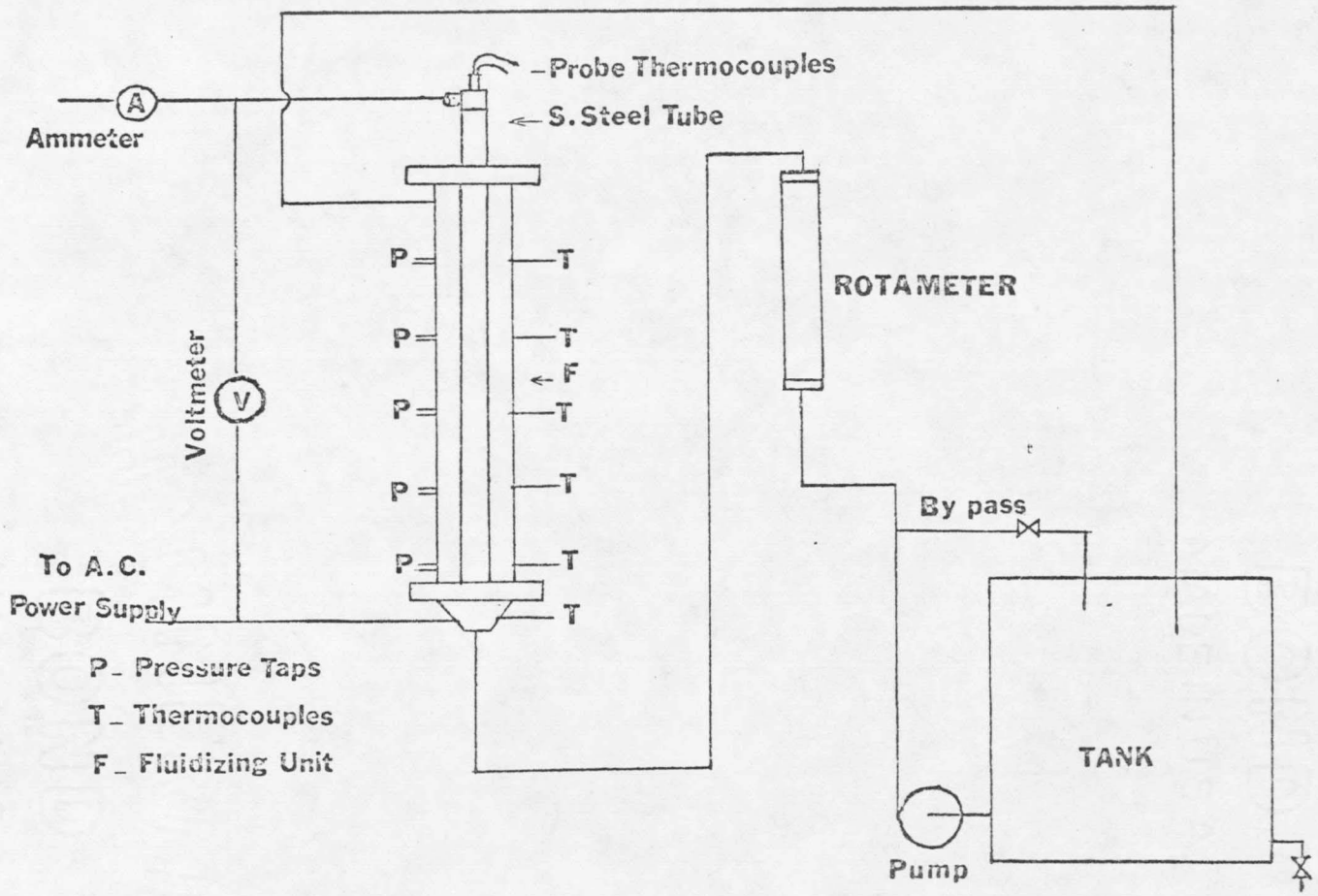

Figure 1. Diagram of equipment.

contacts were made at the top and bottom of the steel tube. A moving thermocouple probe was arranged to run through the center of the steel tube. This probe was attached to a metal rod, used to move the probe up and down. A thermocouple was placed in the fluid intake section to measure the inlet fluid temperature. Five thermocouples and thermocouple shields were mounted at 1.5, 5.5, 9.5, 13.5, and 17.5 inches from the bottom. The thermocouple shield consisted of 0.3 inch diameter, 0.3 inch high cylinder made of fine wire mesh. Five pressure taps were located at 1 1/2-inches from the bottom of the tube and every 4 inches thereafter along the length of the tube.

The stainless steel tube was the heating device. The wall temperature was measured by one moving thermocouple probe inside the heating element.

A centrifugal pump was used to pump water from the tank through the fluidized unit. A bypass was provided to control the flow rate. Water flow rate was measured by a rotameter located in the water supply line. The rotameter was calibrated. Details of this calibration are given in Appendix B.

The Alternating Current Power Supply

The alternating current power supply was made from the supply lines through a step-down transformer. The resistance in the circuit was adjusted so that the current was about 30 to 45 amperes. The emf and current were measured by an AC Voltmeter with a range from zero to five

volts and an AC Ammeter with a range from zero to fifty amperes. The meters were quoted by the manufacturers to be accurate within ± 2 percent.

Measuring Devices

The pressure drop across the bed was measured by a manometer system using carbon tetrachloride fluid with a specific gravity of 1.584.

The wall temperature was measured at various positions by a thermocouple probe which moved up and down inside the tube wall. A thermocouple was embedded in each contact and was electrically insulated from the copper. Each copper contact was held in contact with the wall by a spring. A detailed description of such a probe was given by Noe and Knudsen (8).

All temperatures were measured with Iron-Constantan thermocouples. The thermocouple emf was read using a Leeds and Northrup Co. potentiometer model 0386100. Thermocouples placed in the bed were used to determine the bulk temperature of the water flowing through. All reference junctions were kept in an ice-bath at 32°F.

A switching system was used to complete the thermocouple circuits.

EXPERIMENTAL PROGRAM AND PROCEDURE

Experimental Program

The objective of this investigation was to determine local and average heat transfer coefficients for transfer of energy from an internally heated tube to water flowing through a fluidized bed at various operating conditions. The experimental program was designed to fulfill this objective.

The variables that are most likely to affect the transfer of energy from an internal surface to a fluidized bed can be catagorized into three groups: (1) properties of the fluidizing medium and fluidized particles, (2) operating conditions and (3) equipment geometry and design.

Variables under consideration in this investigation are: particle concentration or static bed height, particle distribution and liquid flow rate. Heat flux, tube wall temperature profile, and vertical bulk liquid temperature were measured in order to calculate the desired coefficients. Bed section pressure drops were measured in order to calculate particle distributions.

Water was used as the fluidizing medium. The water used was approximately at the same temperature for all runs which made it possible to keep the thermal conductivity, heat capacity, viscosity and density of the fluid constant.

Properties of the Particles

Three types of particles were used in this investigation: (1) glass spheres, manufactured by the Minnesota Mining and Manufacturing Company, of 0.0185 inch average diameter; (2) stainless steel particles, manufactured by the Hoeganaes Corporation, Riverton, N.J., of 0.014 inch average diameter; and (3) coke particles of 0.014 inch average diameter. The densities of the glass, stainless steel and coke particles are 156 lb/ft^3, 488 lb/ft^3 and 138 lb/ft^3, respectively. It can be seen from Figure 2 that the glass particles are spherical, whereas the coke and stainless steel particles are somewhat irregular in shape.

Particle Concentration and Distribution

Static bed heights of six and nine inches were investigated for the three types of particles. Data were also taken without particles in the system in order to compare with data reported in literature.

Fluid Mass Velocity

The fluid mass velocities were restricted to the low velocity region. The mass velocity ranged from 2,960 to 32,650 $lb/hr.ft.^2$ Different possible flow rates were investigated at each static bed height. The first rate was chosen near the minimum fluidizing velocity and thereafter the rate was increased.

Experimental Procedure

The following preliminary procedure was performed before each experimental run:

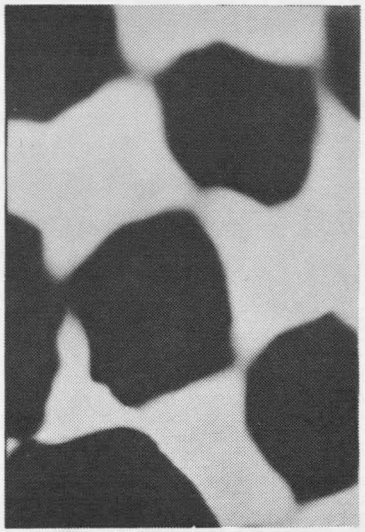

Coke Particles

Stainless Steel Particles

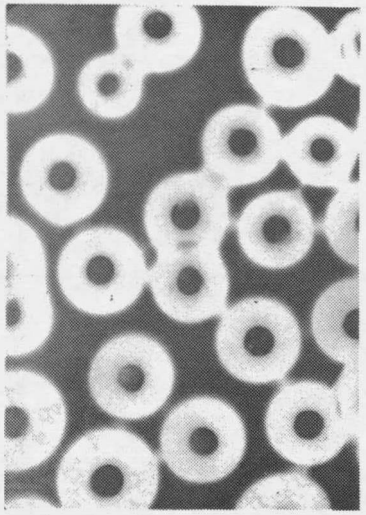

Glass Particles

Figure 2. Photographs of Particles

1. The desired amount of particles was placed in the bed. The water pump was turned on and the bypass valve adjusted to give the desired flow rate.

2. A thermos flask was filled with crushed ice and water. The thermocouple reference junctions were placed in the flask to give a reference temperature of 32°F.

3. The potentiometer was balanced against the internal standard cell.

4. The tube wall probe thermocouple was set to its initial position.

5. The power supply was turned on.

6. When steady state was observed with regard to tube wall thermocouple emf, the recording of data commenced.

The following procedure was used in recording the necessary data:

1. The tube wall emf was measured with the potentiometer. The probe was then placed in the second position and the probe allowed to attain steady state. The same procedure was continued until all five probe positions were measured.

2. When the probe was coming to steady state between probe emf measurements, the remaining data were taken. The current, voltage, water inlet temperature, five bulk liquid temperatures, rotameter reading and bed pressure drops were recorded at five equal time intervals during the course of the run.

After all the data were recorded for one run, the equipment was turned off, or the procedure was repeated for another run.

In this manner, data were taken for the different solid particles, two bed heights, and water flow rates. A typical data sheet can be found in Appendix C.

CALCULATIONS

Calculations of the following quantities were made: temperatures, local temperature differences, heat flux, local heat transfer coefficients, average heat transfer coefficient, and bed section pressure drops, from the original data. Bed section void fractions and bed section average heat transfer coefficients were calculated from the above calculated data. The calculations were performed with a desk calculator.

The temperatures were obtained from thermocouple emf temperature charts made for standard Iron-Constantan thermocouples with reference junction at 32°F. The local temperature difference was then calculated from the following equation:

$$\Delta T_{loc} = T_w - T_b \tag{17}$$

The heat flux was calculated by determining the power dissipated in the heating element. The product of measured current and voltage drop gives the power dissipated in the heating element. The expression used for the heat flux was:

$$q = 8.348\ VI \tag{18}$$

The local heat transfer coefficient was calculated as follows:

$$h_{loc} = q/\Delta T_{loc} \tag{19}$$

To calculate an average heat transfer coefficient, an integral average temperature difference was used as is cited by Leva (7), i.e.

$$\Delta T_{av} = \frac{1}{L} \int_{o}^{L} \Delta T_{loc}\, dz \qquad (20)$$

This integral was graphically evaluated. The average heat transfer coefficient was then calculated as follows:

$$h_{av} = q/\Delta T_{av} \qquad (21)$$

The flow rate was read from rotameter calibration chart, (see Appendix B).

The pressure drop over the four, 4-inch sections of the fluidized bed was measured with the manometer using a manometer fluid having a specific gravity of 1.584. The following equation gives the pressure drop:

$$\Delta P_b = \frac{\Delta h \quad 62.4(1.584 - 1.0)}{30.5} \quad \frac{g}{g_c} \qquad (22)$$

where: Δh = the manometer reading in centimeters. The following equation was used to calculate bed voidage.

$$(1-\varepsilon) = \frac{\Delta P_b}{L(\rho_s - \rho_\ell)} \quad \frac{g}{g_c} \qquad (23)$$

ANALYSIS OF DATA

Average Nusselt Numbers Without Fluidization

Data were taken without fluidization for laminar flow heat transfer in the annulus. Arithmetic mean Nusselt numbers calculated were compared with the correlation suggested by Chen, et al, (1) in the following form:

$$Nu_{a.m.} = 1.02(Re)^{0.45}(Pr)^{\frac{1}{3}}\left(\frac{\mu_a}{\mu_w}\right)^{+0.14}\left(\frac{D}{L}\right)^{+0.4}\left(\frac{D_1}{D_2}\right)^{0.8}(Gr)^{0.05} \qquad (24)$$

(Re based on equivalent diameter, D_e.)

where μ_a is the viscosity at the arithmetic mean bulk temperature of the fluid and μ_w is the viscosity at the temperature T_i of the inner wall of the annulus.

The experimental data were within 45% of Equation 24, as seen in Figure 3. It was noticed that the Nusselt number had a Reynolds number dependency similar to that suggested by this correlation. However, the high value of coefficients could be attributed to the lower ratio of the equivalent diameter to the length in this equipment and to the entrance effects.

Local Heat Transfer Coefficients

Local heat transfer coefficients are measured at distances of 1.5, 5.5, 9.5, 13.5, and 17.5 inches from the entrance of the tube. The calculated local heat transfer coefficients are plotted versus the distance from the entrance for each static bed height used, with mass velocity as the parameter.

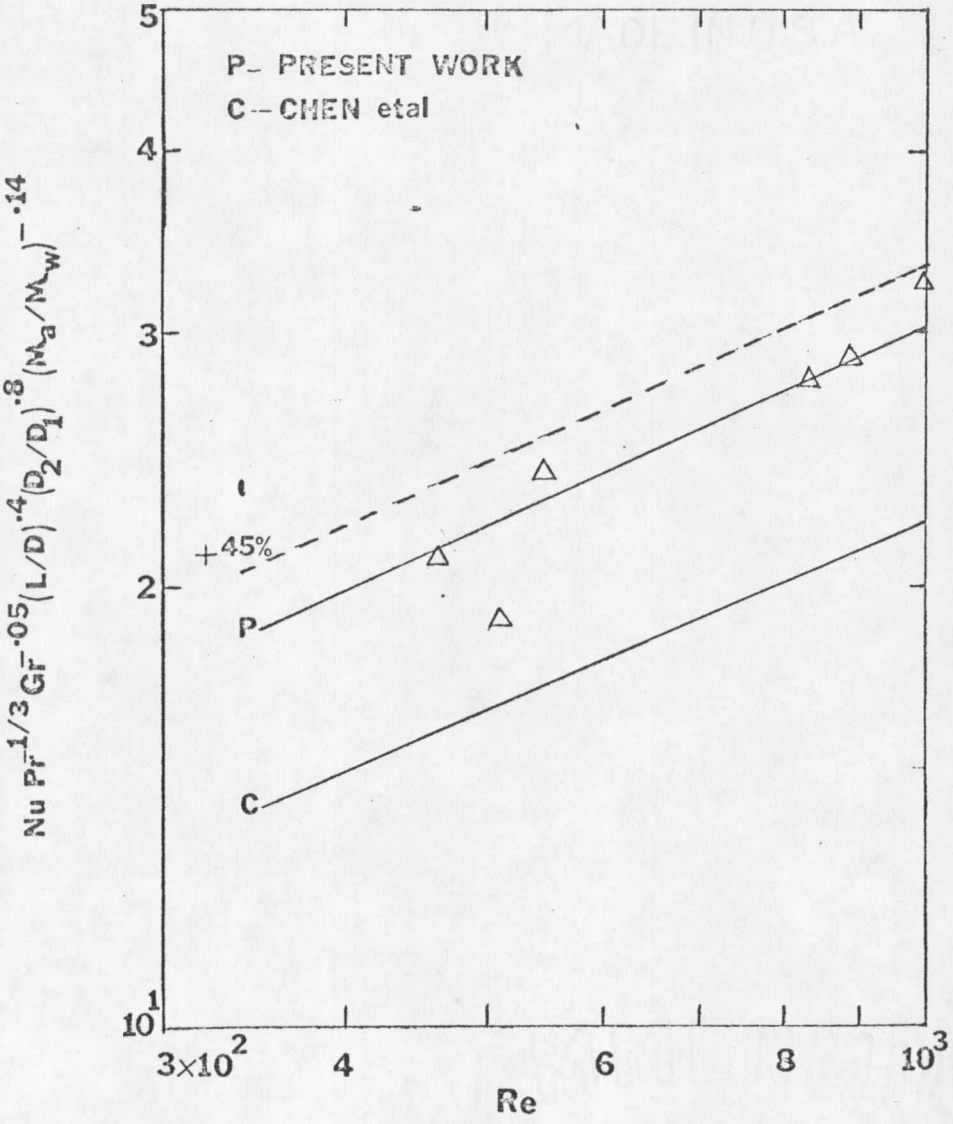

Figure 3. Average Nusselt Numbers for Laminar Flow in the Annulus

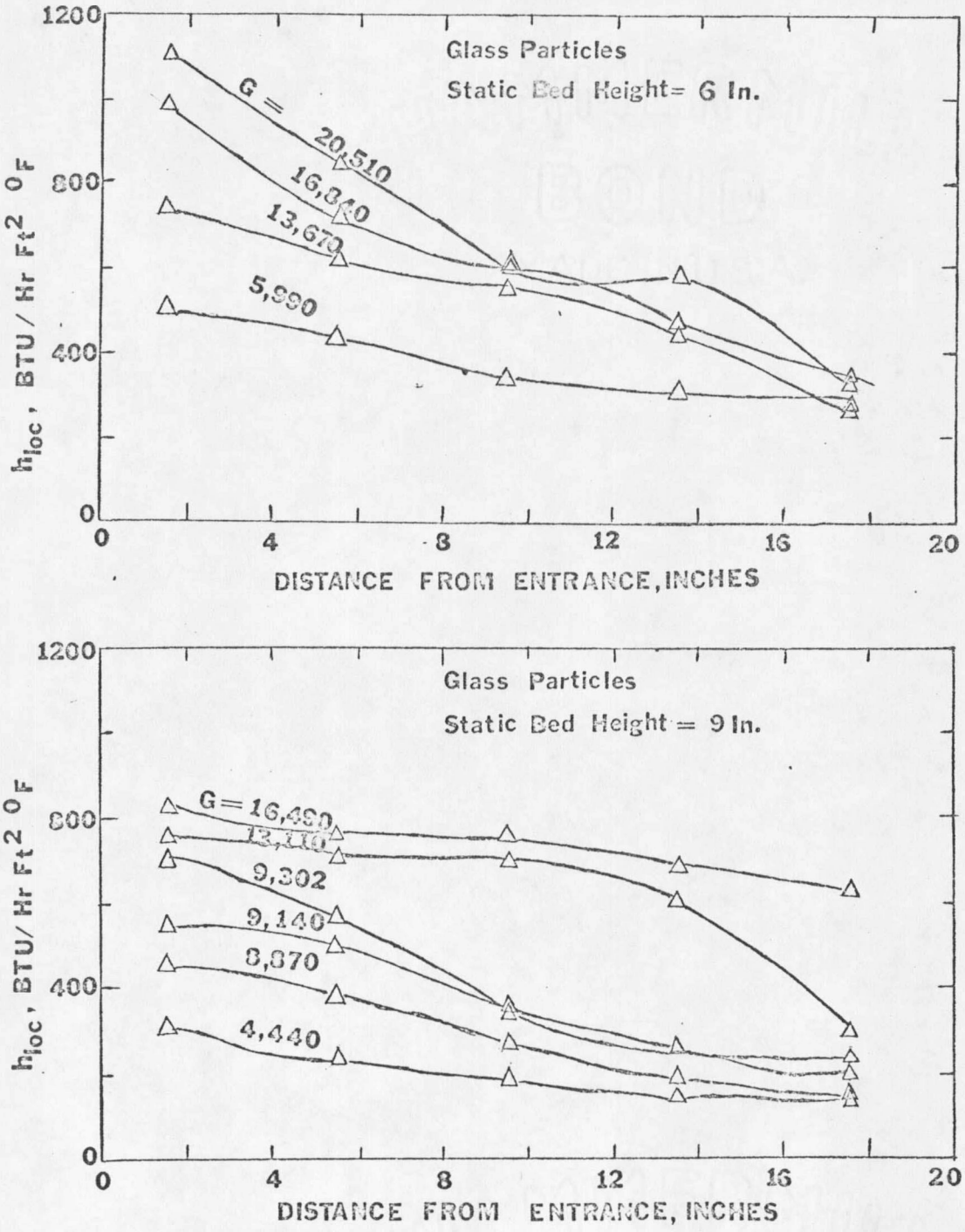

Figure 4. Local Heat Transfer Coefficients for Fluidization, Glass Particles.

Local heat transfer coefficients versus distance from the entrance are plotted in Figure 4 for the glass particles. A progressive increase in heat transfer coefficient is observed with increasing velocity. For For a static bed height of nine inches, the increase is less in the upper three positions, up to G = 9302, because in that part there is no fluidization. However, rapid increase in the heat transfer coefficient is observed at these positions also when the entire section is fluidized.

In Figure 5, local heat transfer coefficients are plotted versus the distance from the entrance for coke. A similar decrease in the heat transfer coefficient with distance is observed. Comparing the heat transfer coefficients for the approximately equal G values for glass and coke particles, it is noted that the coefficients are higher with coke particles than with glass particles. This would be expected for the following reasons: coke particles are less dense, they are smaller in diameter, and more irregular in shape.

Figure 6 shows the plot of local heat transfer coefficients for stainless steel particles. Less increase in the coefficient in the upper two positions is noticed with the six inch static bed height, as this portion of the tube is not fluidized. Comparison with coefficients obtained at same G for glass and stainless steel reveals that the heat transfer coefficients are up to two times higher for stainless steel particles. This could be attributed to the fact that they are small in diameter and highly irregular in shape.

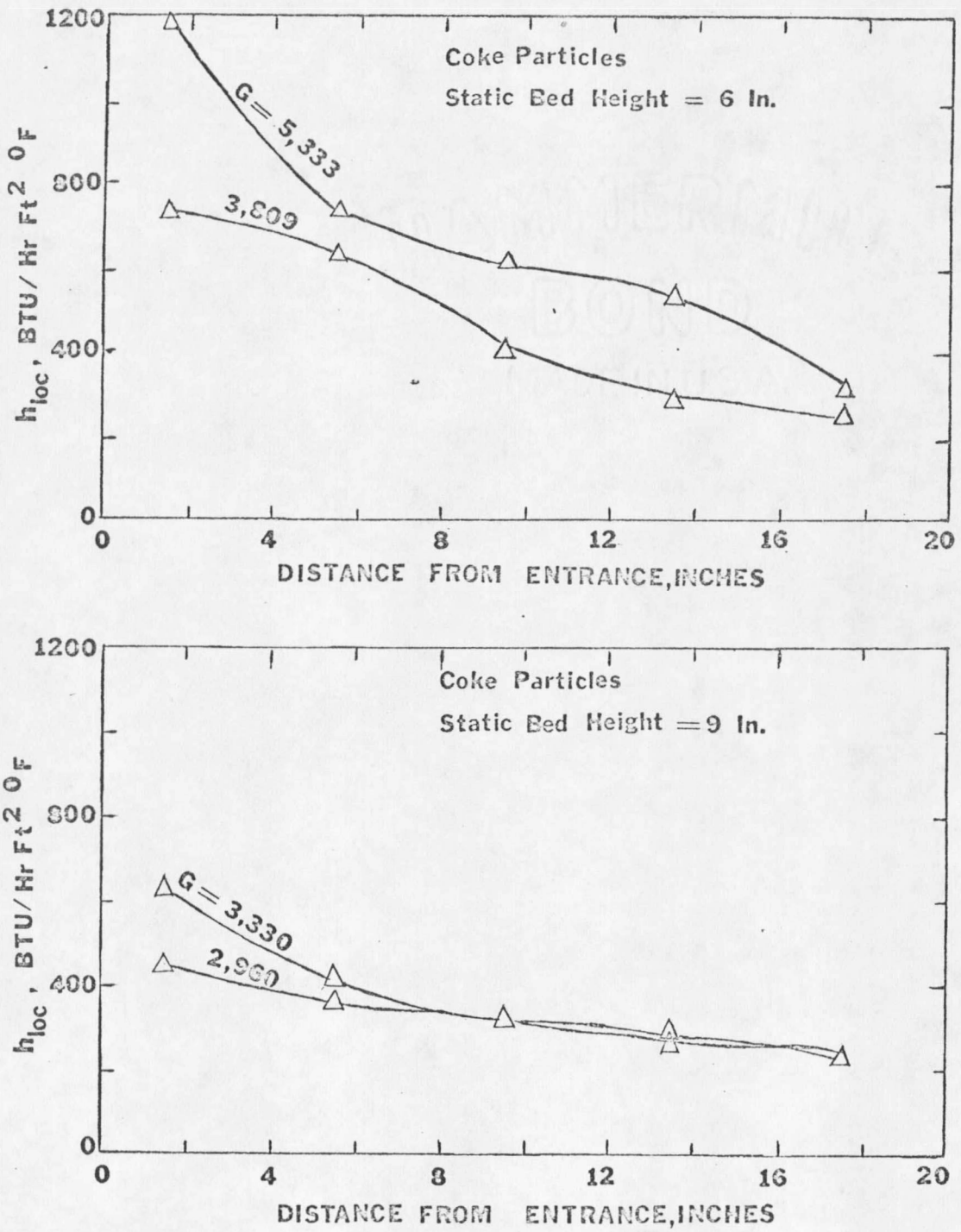

Figure 5. Local Heat Transfer Coefficients for Fluidization, Coke Particles.

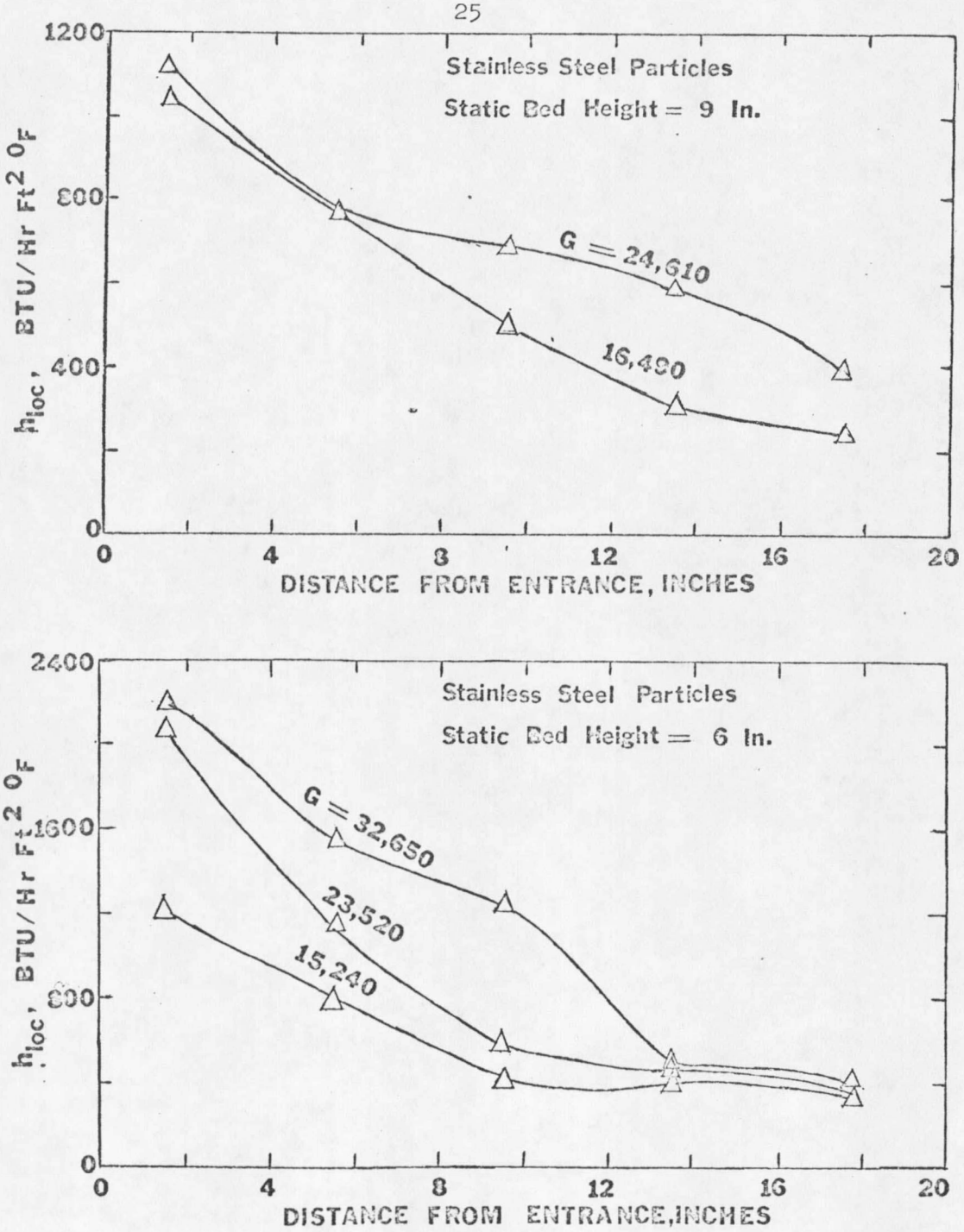

Figure 6. Local Heat Transfer Coefficients for Fluidization, Stainless Steel Particles.

Average Coefficients With Fluidization

With experimentally determined average particle fractions and average Nusselt numbers over the section of the fluidized bed, average particle contact time, $\bar{\theta}$, was calculated from Equation 14. Calculated contact times averaged 0.1, 0.087, and 0.17 seconds for glass spheres, coke particles, and stainless steel particles, respectively. Comparison of these is not possible because no work has reported these values. However, these values are comparable to those obtained by Genetti (2,3) for gas fluidization.

To obtain a correlation for the contact time, $\bar{\theta}$, the dimensionless groups $\bar{\theta}\, g^{1/2} D_p^{-1/2}$, ρ_s/ρ_ℓ and Re_p were calculated. These quantities are plotted on logarithm scales in Figure 7. The following correlation, developed by least square analysis, represents the data:

$$\bar{\theta}\,\left(\frac{g}{D_p}\right)^{1/2}\left(\frac{\rho_\ell}{\rho_s}\right)^{0.8} = 17(Re_p)^{-0.43} \tag{25}$$

By substituting $\bar{\theta}$ as expressed in Equation 16 the following correlation for average Nusselt numbers can be obtained:

$$Nu_p = \frac{2\,\phi\,(1-\varepsilon)^{-0.85}}{\left[1 + \frac{102}{Re_p^{+0.43}}\left(\frac{K_\ell}{\rho_s C_s\, g^{1/2} D_p^{3/2}}\right)\left(\frac{\rho_s}{\rho_\ell}\right)^{0.8}\right]^2} \tag{26}$$

where: ϕ is the ratio of the surface area of the particle to the surface area of a sphere of the same average diameter.

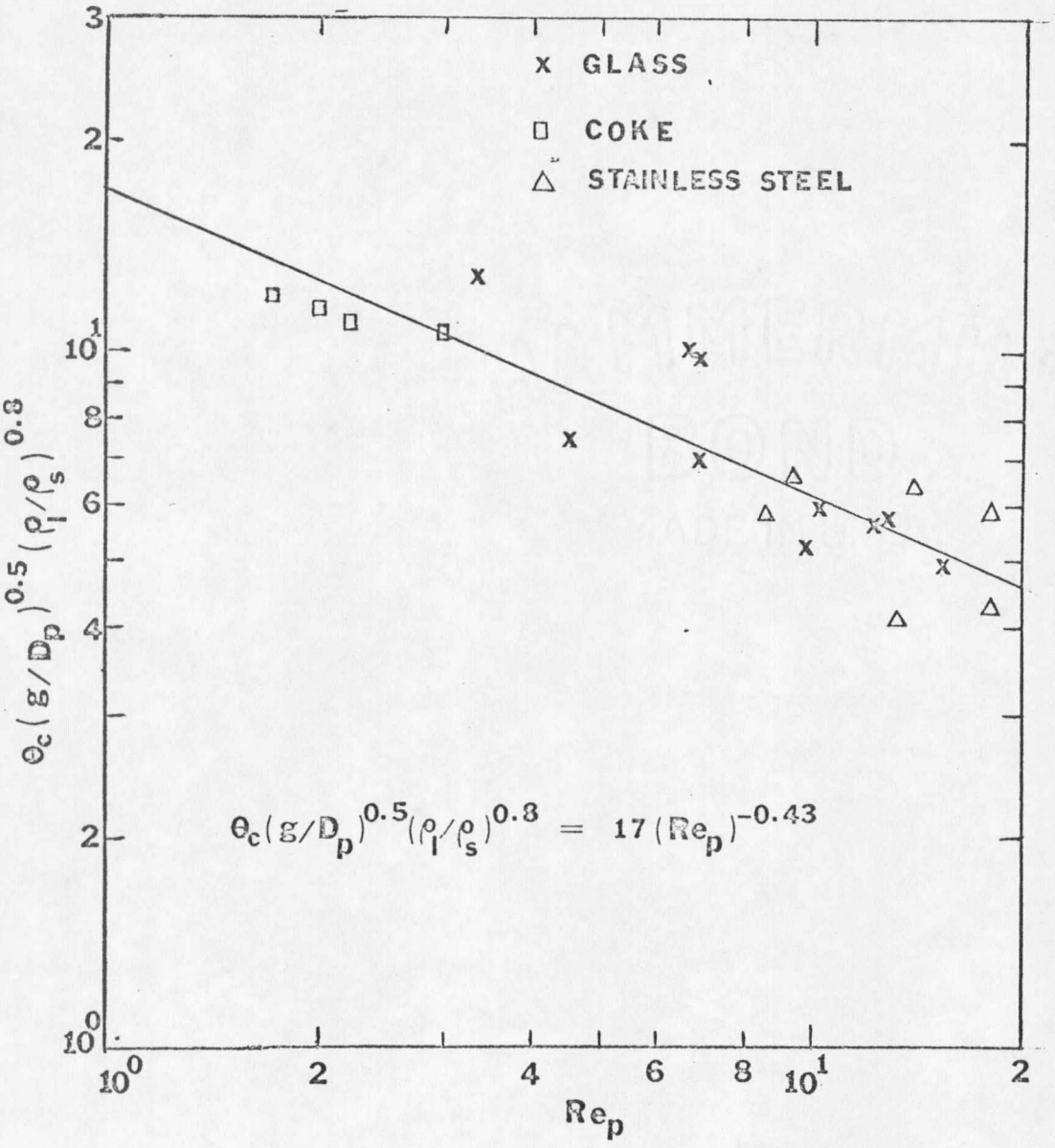

Figure 7. Correlation for Average Contact Time.

Microscopic enlargement, (see Figure 2), of coke and stainless steel particles, shows irregularity in shape with cracks on the surface. As a result of this observation the value of $\phi = 2$ was assumed for coke and stainless steel particles. For the spherical glass particles $\phi = 1$ was used. Equation 26 and the experimental data are shown in Figure 8. Most of the data are within $\pm$ 25 per cent of Equation 26. The scatter is attributed to the less accurate measurement of temperature drops in the bed as the heat fluxes obtained were small, thus making the ΔT's small.

Comparison With Caldas and Lemlich's Correlation

The present data were compared with the correlation proposed by Lemlich and Caldas (6). For low velocity regimes they have correlated with particle Nusselt numbers with the following equation:

$$Nu_p = 0.055\ Re_p \tag{3}$$

Equation 3, together with the present data is plotted in Figure 9. A greater slope than predicted by Caldas and Lemlich has been observed in the plot of the particle Reynolds number versus particle Nusselt number. This could be attributed to the fact that the geometry of the equipment used by Caldas was different from the present investigation. Richardson and Mitson (9) also observed that the heat transfer coefficients obtained by Caldas were low.

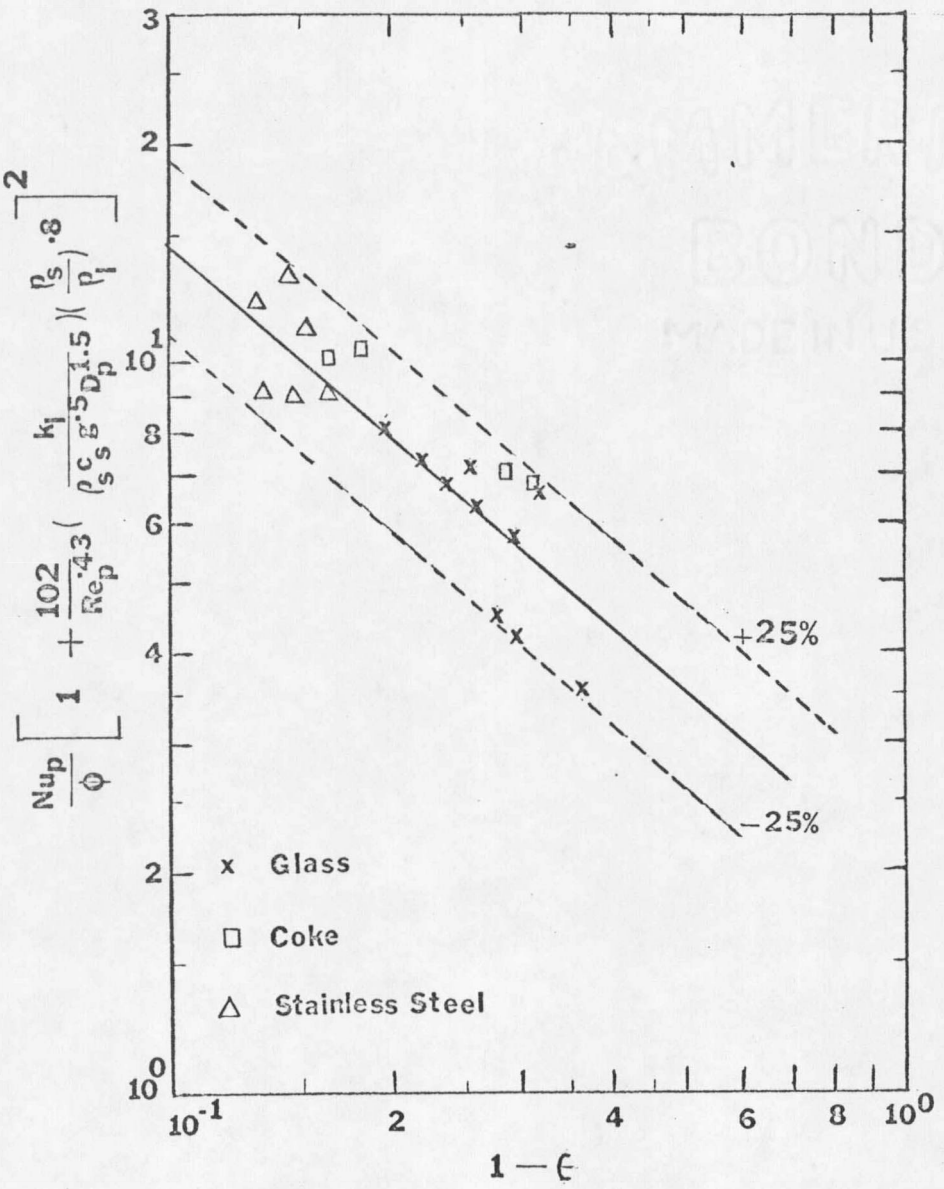

Figure 8. Correlation of Average Nusselt Numbers.

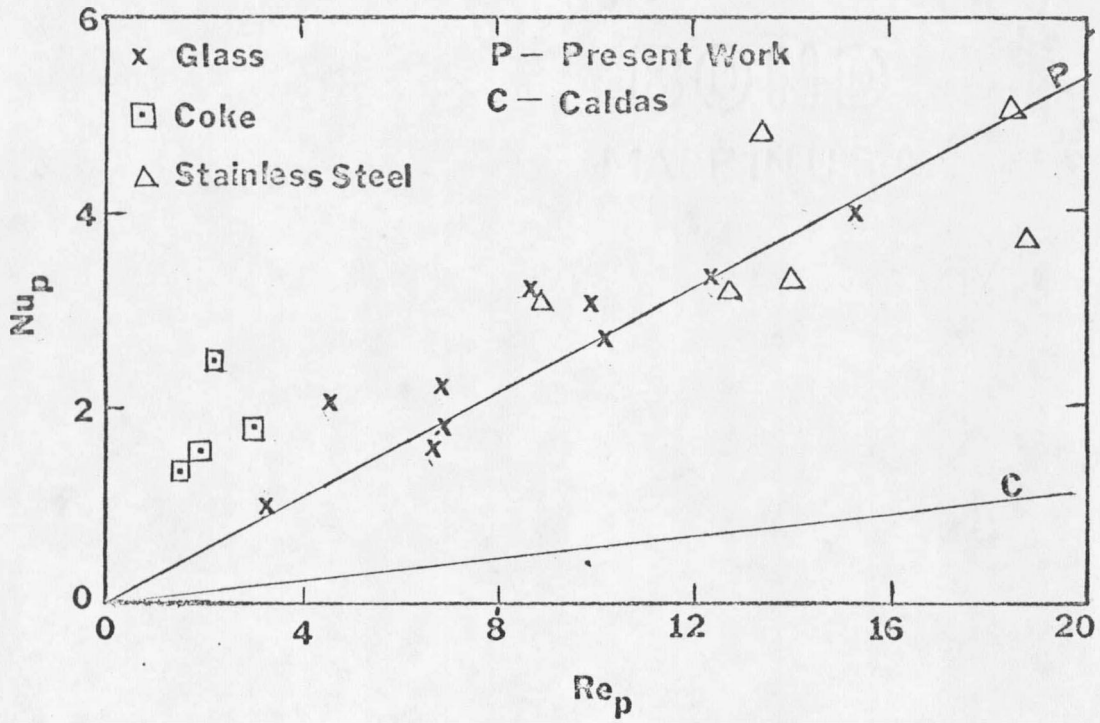

Figure 9. Comparison of Average Nusselt Numbers with Caldas' Correlation.

RESULTS AND CONCLUSIONS

Local and average heat transfer coefficients for heat transfer from the inner wall surface to the fluidized bed in the annulus were investigated. Water was used as the fluidizing medium and glass spheres, coke particles and stainless steel particles were fluidized in the annulus. Heat transfer coefficients for water flowing through the annulus without fluidization were also investigated.

Average Nusselt Numbers Without Fluidization

The average heat transfer coefficients for water alone have the predicted Reynold's number dependency as in the literature (1); therefore, it is concluded that reasonably correct values of coefficients were obtained by the procedure followed.

Local Heat Transfer Coefficients

Local heat transfer coefficients are observed to decrease with the distance from the entrance of the bed. With coke and stainless steel particles the local heat transfer coefficients are higher than with glass spheres, owing to their irregular shape.

Average Heat Transfer Coefficients

Nusselt numbers averaged over the fluidized bed are correlated with Equation 26, an equation developed from a form of the Ziegler, Koppel and Brazelton model (12); Genetti and Knudsen (3) for fluidized bed heat transfer, i.e.,

$$Nu_p = \frac{2\,\phi\,(1-\varepsilon)^{-0.85}}{\left[1 + \frac{102}{Re_p} + 0.43\left(\frac{K_\ell}{\rho_s C_s D_p^2}\right)\left(\frac{\rho_s}{\rho_\ell}\right)^{0.8}\left(\frac{D_p}{g}\right)^{1/2}\right]^2} \qquad (27)$$

The following conclusions can be drawn from this correlation:

1. Particle Nusselt numbers are independent of particle thermal conductivity.

2. Particle Nusselt numbers are proportioned to $(1-\varepsilon)^{-0.85}$.

3. Particle Nusselt numbers are dependent on particle surface area.

APPENDIX A

NOMENCLATURE

Symbol	Definition	Dimensions
C_f	heat capacity of the fluid	Btu/lb_m °F
C_ℓ	heat capacity of water	Btu/lb_m °F
C_s	heat capacity of solids	Btu/lb_m °F
D_e	equivalent diameter of the annulus	ft.
D_p	particle diameter	inches, ft.
emf	electro motive force produced by the thermocouples	millivolts
F_e	velocity correction factor of Equation 2	dimensionless
g	acceleration due to gravity	ft/sec^2
g_c	gravitational constant	$\frac{lb_m ft.}{lb_f sec^2}$
G	liquid mass velocity	$lb_m/hr.ft.^2$
h	heat transfer coefficient	Btu/$hr.ft.^2$°F
h_{loc}	local heat transfer coefficient	Btu/$hr.ft.^2$°F
Δh	manometer readings	cm.
I	current flowing through the heating element	amperes.
K_ℓ	thermal conductivity of water	Btu/hr.ft.°F
K_s	thermal conductivity of solid	Btu/hr.ft.°F
L	length of fluidized bed	ft.
M	defined by $\frac{12 K_\ell}{P_s C_s D_p^2}$ in Equation 6a	dimensionless
Nu_p	particle Nusselt number, $\frac{h D_p}{K_\ell}$	dimensionless

NOMENCLATURE Cont.

Symbol	Definition	Dimensions
Nu_{av}	average particle Nusselt number, $\frac{h_{av} D_p}{K_\ell}$	dimensionless
ΔP_b	pressure drop across the fluidized bed	$lb_f/ft.^2$
q	heat flux from heat transfer surface	$Btu/hr.ft.^2$
q_p	heat flux to a particle near the heat transfer surface	$Btu/hr.ft.^2$
Re	Reynolds number	dimensionless
Re_p	particle Reynolds number, $\frac{D_p G}{\mu}$	dimensionless
T	temperature	^oF
T_b	bulk bed liquid temperature	^oF
T_w	tube wall temperature	^oF
ΔT_{loc}	local temperature difference	^oF
ΔT_{av}	average temperature difference	^oF
V	voltage drop across heating element	Volts
γ_p	number of particles per unit surface area	$particles/ft.^2$
ε	void fraction	dimensionless
θ	contact time	hr.
$\bar{\theta}$, θ_c	average contact time	hr.
ρ_ℓ	density of liquid	$lb_m/ft.^3$
ρ_s	density of solid	$lb_m/ft.^3$
μ	viscosity of liquid	$lb_m/hr.ft.$
ϕ	ratio of the particle surface area to the area of a spherical particle of the same diameter	dimensionless

APPENDIX B

CALIBRATION OF THE ROTAMETER

The rotameter was calibrated by measuring flow rates at known values of rotameter readings by the following procedure: the flow rate was adjusted to a constant rotameter reading. The flow rate was measured at the outlet by collecting a known amount of water. The flow rate was changed to a different reading and the time taken for a known amount of volume of water was noted. The resulting calibration chart is shown in Figure 10. The plot is rotameter reading vs. flow rate, gallons per minute.

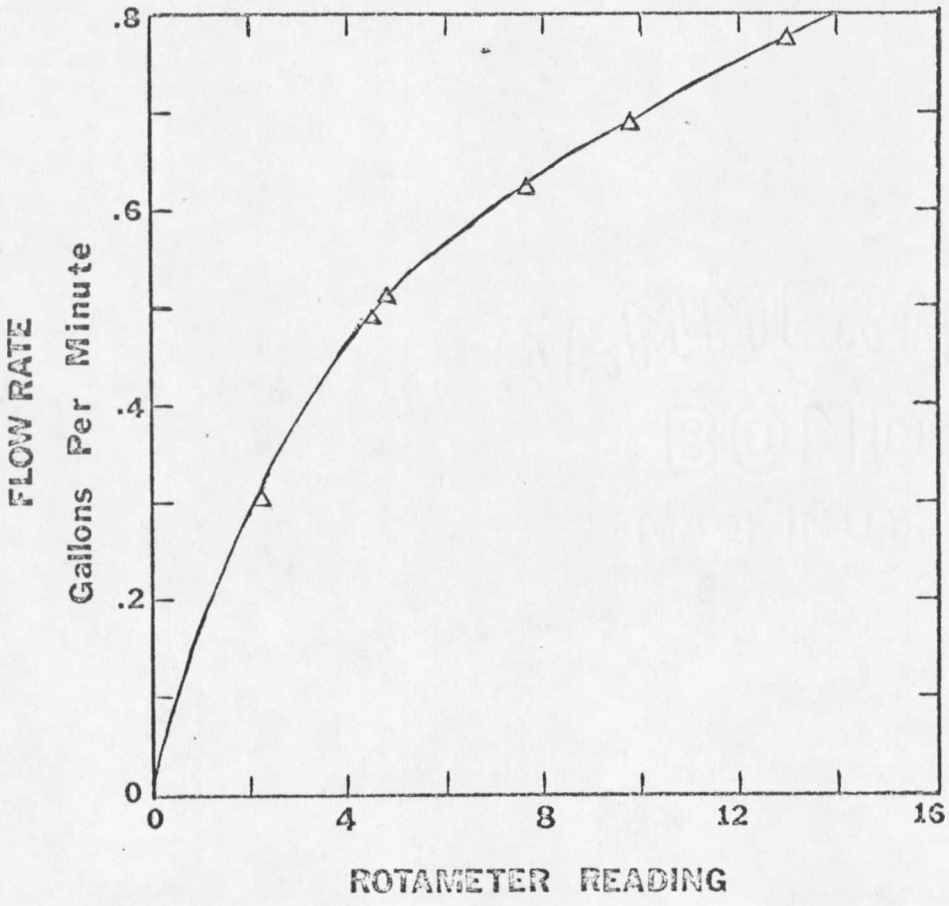

Figure 10. Rotameter Calibration Data

APPENDIX C

SAMPLE RAW DATA SHEET

Run 3D

Date: May 17, 1969

Type of particle: Glass
Static bed height: 6 inches

Expanded bed height: 11 inches

Voltmeter reading, volts	4.45	4.45	4.45	4.45	4.45
Ammeter reading, amperes	41.5	42.0	42.0	42.0	42.0
Rotameter reading	4.7	4.7	4.7	4.6	4.8
Inlet thermocouple emf, mv.	1.42	1.42	1.425	1.42	1.42
Manometer			Cm of CCl_4		
Manometer 1, Δh	7.0	7.0	7.0	7.0	7.0
Manometer 2, Δh	6.7	6.7	6.7	6.8	6.7
Manometer 3, Δh	4.0	4.0	4.0	4.0	4.0
Manometer 4, Δh	0.2	0.2	0.2	0.2	0.2
Tube wall probe thermocouples					
position in.	1.5	5.5	9.5	13.5	17.5
	mv.	mv.	mv.	mv.	mv.
emf 1	1.600	1.550	1.520	1.510	1.500
emf 2	1.585	1.540	1.500	1.500	1.495
Bulk bed thermocouples emf	mv.	mv.	mv.	mv.	mv.
height inches. 1.5	1.420	1.425	1.430	1.435	1.434
5.5	1.425	1.430	1.430	1.430	1.435
9.5	1.425	1.425	1.425	1.430	1.430
13.5	1.423	1.425	1.427	1.427	1.428
17.5	1.425	1.425	1.426	1.427	1.427

APPENDIX D

Table I. Experimental and Calculated Data

RUN 2C GLASS SPHERES STATIC BED HEIGHT = 9 inches

Probe Location (inches)	Tube Wall Temperature (°F)	Temperature Difference (°F)	Local Heat Transfer Coefficient (Btu/hr.sq.ft.°F)
1.5	88.8	2.1	454
5.5	88.4	2.4	397
9.5	89.3	3.4	280
13.5	90.3	5.0	191
17.5	91.3	6.0	159

Heat Flux = 955 Btu/hr.sq.ft. Average Heat Transfer Coefficient = 367 Btu/hr.sq.ft.°F.

RUN 2D GLASS SPHERES STATIC BED HEIGHT = 9 inches

1.5	77.0	1.6	718
5.5	77.5	2.0	575
9.5	78.8	3.05	377
13.5	79.6	4.2	273
17.5	80.0	4.7	244

Heat Flux = 1150 Btu/hr.sq.ft. Average Heat Transfer Coefficient = 413 Btu/hr.sq.ft.°F.

RUN 2E GLASS SPHERES STATIC BED HEIGHT = 9 inches

1.5	78.2	1.5	764
5.5	78.6	1.55	738
9.5	78.85	1.60	715
13.5	78.9	1.60	602
17.5	80.0	3.7	309

Heat Flux = 1145 Btu/hr.sq.ft. Average Heat Transfer Coefficient = 710 Btu/hr.sq.ft.°F.

RUN 2F GLASS SPHERES STATIC BED HEIGHT = 9 inches

Probe Location (inches)	Tube Wall Temperature (°F)	Temperature Difference (°F)	Local Heat Transfer Coefficient (Btu/hr.sq.ft.°F)
1.5	79.17	1.37	833
5.5	79.17	1.47	777
9.5	79.20	1.50	760
13.5	79.25	1.65	693
17.5	79.25	1.80	635

Heat Flux = 1145 Btu/hr.sq.ft. Average Heat Transfer Coefficient = 760 Btu/hr.sq.ft.°F.

RUN 2H GLASS SPHERES STATIC BED HEIGHT = 9 inches

1.5	91.0	4.0	307
5.5	92.0	5.4	225
9.5	92.35	6.35	192
13.5	93.0	7.4	164
17.5	93.3	7.9	154

Heat Flux = 1220 Btu/hr.sq.ft. Average Heat Transfer Coefficient = 235 Btu/hr.sq.ft.°F.

RUN 2I GLASS SPHERES STATIC BED HEIGHT = 9 inches

1.5	88.7	2.2	554
5.5	88.4	2.4	510
9.5	89.3	3.4	358
13.5	90.3	5.0	244
17.5	91.3	6.0	203

Heat Flux = 1220 Btu/hr.sq.ft. Average Heat Transfer Coefficient = 510 Btu/hr.sq.ft.°F.

RUN 3A GLASS SPHERES STATIC BED HEIGHT = 6 inches

Probe Location (inches)	Tube Wall Temperature (°F)	Temperature Difference (°F)	Local Heat Transfer Coefficient (Btu/hr.sq.ft.°F)
1.5	82.20	2.20	496
5.5	82.45	2.45	446
9.5	82.50	3.10	352
13.5	82.75	3.45	316.8
17.5	82.90	3.80	287.6

Heat Flux = 1093 Btu/hr.sq.ft. Average Heat Transfer Coefficient = 475 Btu/hr.sq.ft.°F.

RUN 3D GLASS SPHERES STATIC BED HEIGHT = 6 inches

1.5	86.35	2.10	742
5.5	84.85	2.55	611
9.5	85.0	2.76	565
13.5	86.2	3.5	445
17.5	88.0	3.8	268

Heat Flux = 1560 Btu/hr.sq.ft. Average Heat Transfer Coefficient = 632 Btu/hr.sq.ft.°F.

RUN 3E GLASS SPHERES STATIC BED HEIGHT = 6 inches

1.5	85.70	1.70	994
5.5	86.05	2.35	719
9.5	86.50	2.80	603
13.5	87.20	3.65	463
17.5	87.40	4.50	375

Heat Flux = 1690 Btu/hr.sq.ft. Average Heat Transfer Coefficient = 742 Btu/hr.sq.ft.°F.

RUN 3F	GLASS SPHERES	STATIC BED HEIGHT = 6 inches	
Probe Location (inches)	Tube Wall Temperature (°F)	Temperature Difference (°F)	Local Heat Transfer Coefficient (Btu/hr.sq.ft.°F)
1.5	86.5	1.5	1104
5.5	87.2	1.9	871
9.5	87.5	2.8	591
13.5	88.0	2.8	591
17.5	89.15	4.65	356

Heat Flux = 1656 Btu/hr.sq.ft. Average Heat Transfer Coefficient = 768 Btu/hr.sq.ft.°F.

RUN 6A	COKE PARTICLES	STATIC BED HEIGHT = 9 inches	
1.5	90.3	2.6	457
5.5	90.9	3.1	382
9.5	91.9	3.6	330
13.5	92.3	4.0	297
17.5	92.9	5.2	228

Heat Flux = 1189 Btu/hr.sq.ft. Average Heat Transfer Coefficient = 417 Btu/hr.sq.ft.°F.

RUN 6C			
1.5	91.7	1.9	632
5.5	92.3	2.8	429
9.5	93.0	3.8	3.6
13.5	93.7	5.0	240
17.5	94.0	5.3	226

Heat Flux = 1202 Btu/hr.sq.ft. Average Heat Transfer Coefficient = 480 Btu/hr.sq.ft.°F.

RUN 7A COKE PARTICLES STATIC BED HEIGHT = 6 inches

Probe Location (inches)	Tube Wall Temperature (°F)	Temperature Difference (°F)	Local Heat Transfer Coefficient (Btu/hr.sq.ft.°F)
1.5	91.0	1.76	735
5.5	91.30	2.0	625
9.5	92.30	3.0	416
13.5	93.10	4.30	290
17.5	93.70	5.0	250

Heat Flux = 1250 Btu/hr.sq.ft. Average Heat Transfer Coefficient = 750 Btu/hr.sq.ft.°F.

RUN 7B COKE PARTICLES STATIC BED HEIGHT = 6 inches

1.5	89.25	1.25	1200
5.5	89.50	1.70	736
9.5	89.70	2.0	626
13.5	90.00	2.30	544
17.5	91.20	3.90	321

Heat Flux = 1252 Btu/hr.sq.ft. Average Heat Transfer Coefficient = 820 Btu/hr.sq.ft.°F.

RUN 9A STAINLESS STEEL PART. STATIC BED HEIGHT = 9 inches

1.5	76.7	1.7	1042
5.5	77.5	2.3	770
9.5	78.8	3.6	492
13.5	81.4	5.9	300
17.5	82.3	7.3	242

Heat Flux = 1773 Btu/hr.sq.ft. Average Heat Transfer Coefficient = 805 Btu/hr.sq.ft.°F.

RUN 9B	STAINLESS STEEL PART.	STATIC BED HEIGHT = 9 inches	
Probe Location (inches)	Tube Wall Temperature (°F)	Temperature Difference (°F)	Local Heat Transfer Coefficient (Btu/hr.sq.ft.°F)
1.5	80.1	1.5	1118
5.5	80.8	2.2	762
9.5	81.4	2.4	698
13.5	81.8	2.8	598
17.5	83.3	4.3	390
Heat Flux = 1677 Btu/hr.sq.ft.		Average Heat Transfer Coefficient = 833 Btu/hr.sq.ft.°F.	
RUN 9C	STAINLESS STEEL PART.	STATIC BED HEIGHT = 9 inches	
1.5	82.06	0.60	2828
5.5	82.30	0.70	2424
9.5	82.85	1.45	1170
13.5	83.50	2.00	848
17.5	84.30	2.70	628
Heat Flux = 1697 Btu/hr.sq.ft.		Average Heat Transfer Coefficient = 1138 Btu/hr.sq.ft.°F.	
RUN 10A	STAINLESS STEEL PART.	STATIC BED HEIGHT = 6 inches	
1.5	83.0	1.3	1242
5.5	83.7	2.0	807
9.5	85.3	3.6	448
13.5	85.7	3.9	419
17.5	86.6	4.9	329
Heat Flux = 1615 Btu/hr.sq.ft.		Average Heat Transfer Coefficient = 978 Btu/hr.sq.ft.°F.	

RUN 10B STAINLESS STEEL PART. STATIC BED HEIGHT = 6 inches

Probe Location (inches)	Tube Wall Temperature (°F)	Temperature Difference (°F)	Local Heat Transfer Coefficient (Btu/hr.sq.ft.°F)
1.5	82.75	0.75	2119
5.5	83.40	1.40	1132
9.5	84.70	2.70	587
13.5	85.30	3.50	453
17.5	86.80	5.00	317

Heat Flux = 1586 Btu/hr.sq.ft. Average Heat Transfer Coefficient = 1468 Btu/hr.sq.ft.°F.

RUN 10C STAINLESS STEEL PART. STATIC BED HEIGHT = 6 inches

1.5	82.7	0.7	2205
5.5	83.0	1.0	1549
9.5	83.2	1.2	1266
13.5	84.8	2.9	532
17.5	85.7	3.8	406

Heat Flux = 1544 Btu/hr.sq.ft. Average Heat Transfer Coefficient = 1544 Btu/hr.sq.ft.°F.

APPENDIX E

Table II. Calculated particle fractions and Nusselt numbers for fluidization.

Run Number	$1-\varepsilon$	Nu_p
Glass Spheres		
2C	0.299	1.60
2D	0.276	1.80
2E	0.254	3.12
2F	0.220	3.34
2H	0.363	1.03
2I	0.292	2.24
3A	0.320	2.08
3D	0.261	2.78
3E	0.223	3.26
3F	0.196	3.98
Coke		
6A	0.321	1.37
6C	0.287	1.58
7A	0.183	2.50
7B	0.164	2.84
Stainless Steel		
9A	0.161	2.65
9B	0.147	3.25
9C	0.131	3.75
10A	0.153	3.22
10B	0.147	4.84
10C	0.132	5.09

LITERATURE CITED

1. Chen, C. Y, G. A. Hawkins, and H. L. Solberg, Trans.ASME, 68, 99(1946)

2. Genetti, W. E., Ph.D. Thesis, Oregon State University, (1968)

3. Genetti, W. E., and J. G. Knudsen, "Heat Transfer in a Fluidized Bed Tubular Heat Exchanger". Accepted for publication in Trans. Inst. Chem. Engrs. (London)

4. Holman, J. P., T. W. Moore, and V. M. Wong, Ind. Eng. Chem. Fundamentals, 4, 21 (1965)

5. Kunii, D., and O. Levenspiel, "Fluidization Engineering", John Wiley, New York (1969)

6. Lemlich, R., I. Caldas, Jr., AIChE J., 4, 376 (1955)

7. Leva, M., "Fluidization", McGraw-Hill, New York (1959)

8. Noe, A. R., and J. G. Knudsen, Chem. Eng. Progr. Symp. Ser. No. 82, 64, 202 (1968)

9. Richardson, J. F., and A. E. Mitson, Trans. Inst. Chem. Engrs. (London), 36, 270 (1958)

10. Sunkoori, N. R., and R. Kaparthi, Chem. Eng. Sci., 12, 166 (1960)

11. Zenz, F. A., and D. F. Othmer, "Fluidization and Fluid-Particle Systems", Reinhold, New York (1960)

12. Zeigler, E. N., L. B. Koppel, and W. T. Brazelton, Ind. Eng. Chem. Fundamentals, 3, 324 (1964)